administration of the nonsustained-release tablet, with the rate decreasing after the 24-hr. point.

The mean equivalent pentylenetetrazol excretion values and the standard deviations for the three groups are given in Table III. Student t values (8) were calculated to compare the mean ^{14}C excretion values of the different groups at various times. Statistically significant ($p = 0.01$) differences were seen between Groups A and B at all collection intervals after the first (0–3 hr.).

No significant differences between Groups A and C were present at any of the collection intervals. These results indicate that urinary excretion of 300 mg. of pentylenetetrazol proceeds at approximately the same rate whether the dose is administered in one sustained-release tablet or divided and administered in three doses at 4-hr. intervals. These results also indicate that the same fraction of pentylenetetrazol was absorbed from the sustained-release tablets as from the nonsustained-release tablets.

There were no significant differences between Groups B and C until the fourth collection (9–12 hr.). Mean excretion values for these two groups were significantly different in all of the last five urine collections.

SUMMARY

Sustained-release and nonsustained-release tablets containing pentylenetetrazol-10-^{14}C were administered to human subjects. The resulting plasma and urine concentrations of equivalent pentylenetetrazol were determined by liquid scintillation counting techniques. Subjects receiving the sustained-release tablets exhibited smoothly sustained plasma levels of equivalent pentylenetetrazol for a period of about 12 hr. and a nearly linear urinary excretion rate of ^{14}C during a period of 36 hr. Subjects receiving three doses of nonsustained-release tablets at 4-hr. intervals exhibited typical rises and falls in plasma ^{14}C levels and an excretion pattern similar to that of the subjects receiving the sustained-release tablets. Subjects receiving a single dose of a nonsustained-release tablet showed one peak plasma ^{14}C level which then decreased continuously. A fairly constant rate of urinary ^{14}C excretion was evident for 24 hr. The results of this study showed that the sustained-release tablet produced absorption and excretion patterns similar to those obtained following three doses of the drug administered in nonsustained-release form at 4-hr. intervals.

REFERENCES

(1) W. R. Ebert, R. W. Morris, and R. L. Bogner, *Del. Med. J.*, **39**, 152(1967).

(2) E. Rosen and J. V. Swintosky, *J. Pharm. Pharmacol.*, **12**, 237T(1960).

(3) J. F. Stiver, J. B. Data, and J. E. Christian, to be published.

(4) J. F. Stiver, Ph.D. thesis, Purdue University, Lafayette, Ind., 1970.

(5) "United States Pharmacopeia," 17th rev., Mack Publishing Co., Easton, Pa., 1965, p. 919.

(6) *Ibid.*, p. 1075.

(7) *Ibid.*, p. 1076.

(8) N. M. Downie and R. W. Heath, "Basic Statistical Methods," 2nd ed., Harper and Row, New York, N. Y., 1965, pp. 138–143, 298.

ACKNOWLEDGMENTS AND ADDRESSES

Received December 31, 1969, from *Philips Roxane Laboratories, Inc., Columbus, OH 43216* and the *Bionucleonics Department, Institute for Environmental Health, Purdue University, Lafayette, IN 47907*

Accepted for publication April 22, 1970.

The authors gratefully acknowledge the assistance of R. C. Anderson, Research and Development Department, Philips Roxane Laboratories, Inc.

* Present address: Research and Development Department, Philips Roxane Laboratories, Inc., Columbus, OH 43216

† Present address: School of Pharmacy, Ferris State College, Big Rapids, MI 49307

‡ Present address: Pathology Department, St. Elizabeth Hospital, Lafayette, IN 47907

§ Present address: Bionucleonics Department, Purdue University, Lafayette, IN 47907

Permeability of Double-Layer Films III

TSUNETO KURIYAMA, MICHIHARU NOBUTOKI, and MICHIO NAKANISHI

Abstract □ Moisture permeability of most double-layer films has a directional property. This "two-sidedness" may be brought about mainly by a change in the permeability coefficient as a result of the change in vapor pressure. To utilize this characteristic, it should be clarified as to how the permeability coefficient varies. For this purpose the differential permeability coefficient was calculated, making it easy to estimate the permeability of moisture under various conditions and making it possible to obtain the distribution of both vapor pressure and the water concentration in double-layer films. When the permeability on single films under various moisture conditions is given, the "two-sidedness" feature of double-layer films made from them will be grasped.

Keyphrases □ Double-layer films—theoretical considerations □ Films, double layer—moisture permeability □ Differential permeability coefficients—double-layer films □ Water concentration, vapor pressure—films

Previous reports (1, 2) dealt with variations of "two-sidedness" in the moisture permeability of double-layer films with changing conditions. It is very important to investigate the cause (or principle) of these phenomena. Rogers *et al.* (3) explained the two-sidedness skillfully, even though they did not classify such characteristics as were reported in a previous report (1). Their theory can be regarded as applicable to understand various types of two-sidedness and their behavior under changing moisture conditions. As stated in a previous report (2), the permeability coefficient, P, is not constant but varies with the moisture changes. Rogers *et al.* (3) introduced the concept of the differential permeability coefficient to solve this problem. The following theoretical considerations are mainly based on these ideas.

EXPERIMENTAL

The experimental method and the abbreviation for each film are the same as those in previous reports (1, 2).

Cell for Measuring Water Vapor Permeability—The cell and measuring method are modifications of those of Patel *et al.* (4). Permeation through a sample film was determined by measuring weight change of the cell at a certain condition.

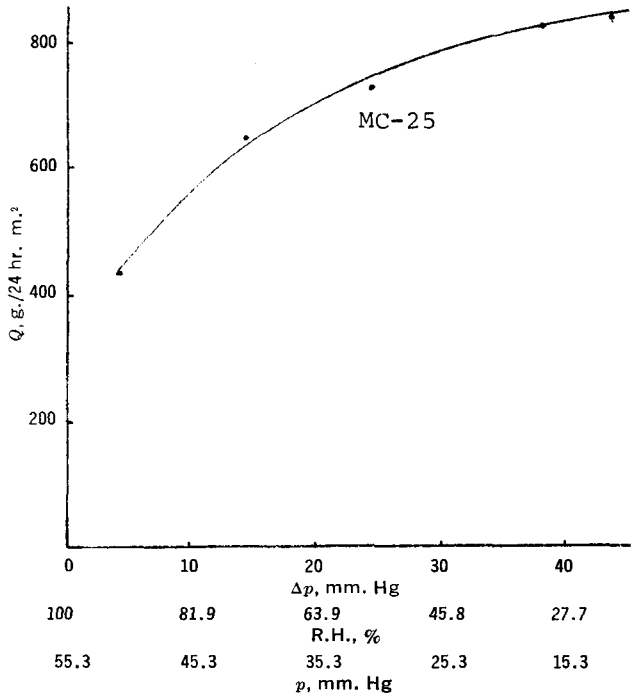

Figure 1—*Relationship between* Q *and* Δp. *Temperature, 40°; thickness of film, 0.2 mm.;* p_1 = *100% R.H. = 55.3 mm. Hg; and* $\Delta p = p_1 - p$.

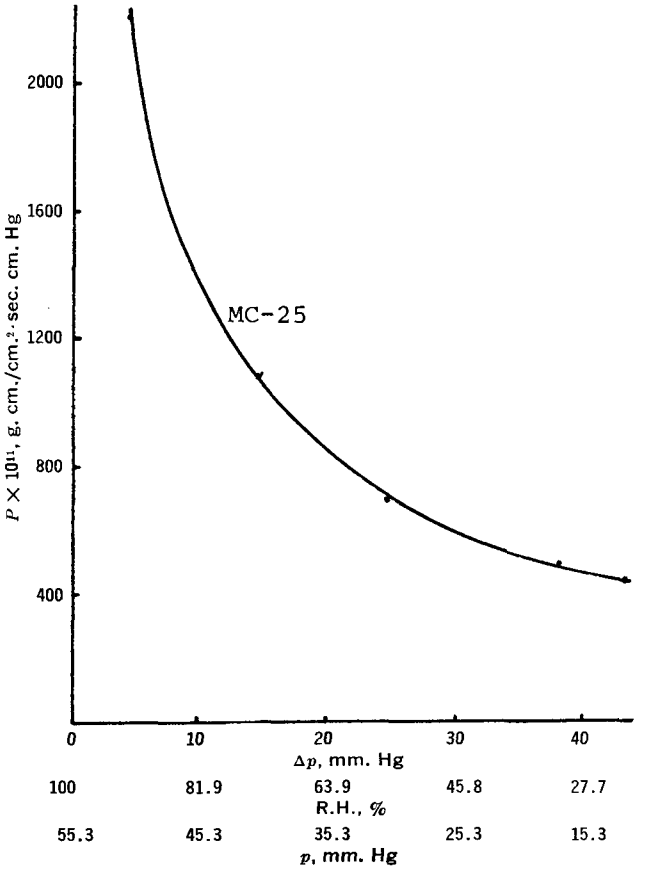

Figure 2—*Relationship between* P *and* Δp. *Temperature, 40°; thickness of film, 0.2 mm.;* p_1 = *100% R.H. = 55.3 mm. Hg; and* $\Delta p = p_1 - p$.

Film Preparation—*Single Film*—Free film was prepared by casting a solution of coating agent on a glass plate.

Double-Layer Film—Two single films were combined to form a double-layer film by using a solvent that dissolved only a surface of either film.

Measurement of Film Thickness—The thickness of a single film is expressed as the mean value of 12 different points measured with a dial gauge (precision 0.001 mm.) in a sample film (4 cm. in diameter). Standard deviation of the thickness in a sample film was less than 0.0006 mm. at 0.05-mm. thickness, 0.0008 mm. at 0.15-mm. thickness, and 0.001 mm. at 0.25-mm. thickness.

Materials—The coating agents used are as follows:

Abbreviation	Chemical Name	Manufacturer (Specification)
EC	Ethylcellulose	Dow Corning (50 cps.)
MC	Methylcellulose	Shin-etsu Chemical Co. (25 cps.)
HECAP	Hydroxyethylcellulose acetate phthalate	Yoshitomi Pharmaceutical Industries (5)

All permeability data were determined as the mean of six observations at the same condition.

RESULTS AND DISCUSSION

Figure 1 shows the relationship between the pressure difference, Δp, and the moisture permeability, Q, across methylcellulose (MC-25) film of 0.2-mm. thickness.

Application of Eq. 1 to this relationship gives the permeability coefficient P. The result is shown in Fig. 2.

$$Q = \frac{q}{At} = P\frac{p_1 - p_2}{l} = P\frac{\Delta p}{l} \qquad \text{(Eq. 1)}$$

where l = thickness of a film, A = permeation area of the film, t = time of permeation, p_1 = water vapor pressure at the side of higher humidity, p_2 = water vapor pressure at the side of lower humidity, P = permeability coefficient of moisture, Q = moisture permeability, and q = quantity of permeated moisture.

Figure 2 shows that the permeability coefficient is not a constant but a function of the humidity condition in which the film is placed. Each section that is rectangular to the direction of permeation across a film may have a certain differential permeability coefficient, depending upon the humidity condition in which the section is located. What is obtained in an experiment is permeability coefficient P, which corresponds to the integrated value of all differential permeability constants involved. This idea is expressed as follows:

$$P = \frac{1}{\Delta p}\int_{p_2}^{p_1} P'\,dp \qquad \text{(Eq. 2)}$$

Table I—Calculation of Differential Permeability Coefficient, p_1 = 5.53 cm. Hg

p, cm. Hg	$\Delta p = p_1 - p$, cm. Hg	Qp_1p, g./24 hr. m.²	$Ql = p\Delta p$, g./sec. cm.	P_{p_1p}, g./sec. cm. cm. Hg	P', g./sec. cm. cm. Hg
5.03	0.5	460	1067×10^{-11}	2134×10^{-11}	
4.93	0.6	485	1125×10^{-11}	1875×10^{-11}	580×10^{-11}
4.83	0.7	506	1174×10^{-11}	1677×10^{-11}	490×10^{-11}
4.73	0.8	528	1225×10^{-11}	1531×10^{-11}	510×10^{-11}
4.63	0.9	550	1276×10^{-11}	1418×10^{-11}	510×10^{-11}

Table II—Calculation of P_{pp_2} (p_2 = 1.03 cm. Hg)

P, cm. Hg	$\Delta p = p - p_2$, cm. Hg	P', g./sec. cm. cm. Hg	$\int_{p_2}^{p} P'\,dp$, g./sec. cm.	P_{pp_2}, g./sec. cm. cm. Hg	Q_{pp_2}, g./24 hr. m.²
1.03	0.0	90×10^{-11}	9×10^{-11}	90×10^{-11}	
1.13	0.1	70×10^{-11}	16×10^{-11}	80×10^{-11}	3.5
1.23	0.2	90×10^{-11}	25×10^{-11}	83×10^{-11}	7.2
1.33	0.3	50×10^{-11}	30×10^{-11}	75×10^{-11}	9.7
1.43	0.4	90×10^{-11}	39×10^{-11}	78×10^{-11}	13.5

where P' is the differential permeability coefficient.

Differentiating Eq. 2 gives Eq. 3:

$$P' = \frac{d(P\,\Delta p)}{dp} \qquad \text{(Eq. 3)}$$

Figure 2 gives the relationship between P and Δp (or p), which may produce P' with the help of Eq. 3. The process of this calculation is summarized in Table I. In this table, each P and Q has a suffix consisting of two letters. The first letter refers to the water-vapor pressure of the side of higher humidity; the second letter refers to the water vapor pressure of the side of lower humidity. For instance, Q_{p_1p} is the Q which is obtained by fixing the water vapor pressure on p_1 at the side of higher humidity and by varying the vapor pressure, p, at the side of lower humidity. In a like manner, the correspondent permeability coefficient of moisture is expressed as P_{p_1p}.

The results shown in Table I were calculated from the data of Fig. 1, not from data of Fig. 2. Although the four values observed in Fig. 2 are converted from Fig. 1, the curve in Fig. 2 is not as accurate as that in Fig. 1, because the former is more sharply curved than the latter. As is understood from Eq. 3, even a small error in P will have a strong influence on the resulting P'. The results obtained in Table I show the relationship that corresponds to the function $P' = f(p)$ under a certain condition. Figure 2 shows the observed values corresponding to Eq. 4. Here, using the relation of $P' = f(p)$ of Table I, P_{pp_2} can be obtained (Eq. 5). P_{pp_2} is the permeability coefficient for varying vapor pressure at the side of higher humidity under constant vapor pressure at the lower side. Moreover, P_{pp_2} gives Q_{pp_2} according to Eq. 1.

$$P_{p_1p} = \frac{1}{p_1 - p}\int_{p}^{p_1} P'\,dp \qquad \text{(Eq. 4)}$$

$$P_{pp_2} = \frac{1}{p - p_2}\int_{p_2}^{p} P'\,dp \qquad \text{(Eq. 5)}$$

These calculations were made in accordance with Table II, and the results are shown in Fig. 3.

P_{p_1p} is considerably different from P_{pp_2}. This means that the moisture permeability will be different when the mean value of vapor pressure is not the same, even if the difference of pressure across the film is constant. The calculated P' values were considerably divergent as plotted in Fig. 3. This divergence was caused, as mentioned previously, by the fact that the values of P' were strongly influenced by the slightest errors of P (errors of observation and plotting). P' values used in Table II are the raw results from Table I, so the P_{pp_2} values obtained are divergent too. However, if the compensated values of P' obtained from the regression curve in Fig. 3 are used, a better curve can be obtained around P_{pp_2}. Rogers *et al.* (3) explained the two-sidedness of the permeability without calculating P'. Their idea shows that it is possible to obtain Q_{pp_2}

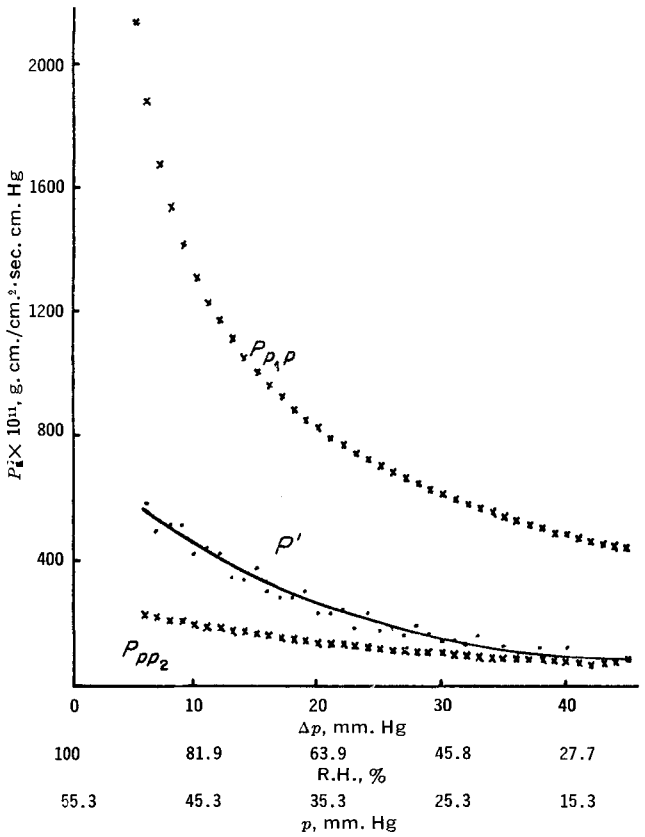

Figure 3—*Δp-profile of* P', P_{p_1p}, *and* P_{pp_2}. *Material, MC-25; thickness of film, 0.2 mm.; temperature, 40°;* p_1 = *100% R.H.* = *55.3 mm. Hg; and* $\Delta p = p_1 - p$. P_{p_1p} = *permeability coefficient observed by fixing the water vapor pressure on* p_1 *at the side of higher humidity and by varying the vapor pressure* p *at the side of lower humidity.* P_{pp_2} = *permeability coefficient calculated fixing the water vapor pressure on* p_2 *at the side of lower humidity and varying the vapor pressure* p *at the side of higher humidity.* P' = *differential permeability coefficient calculated.*

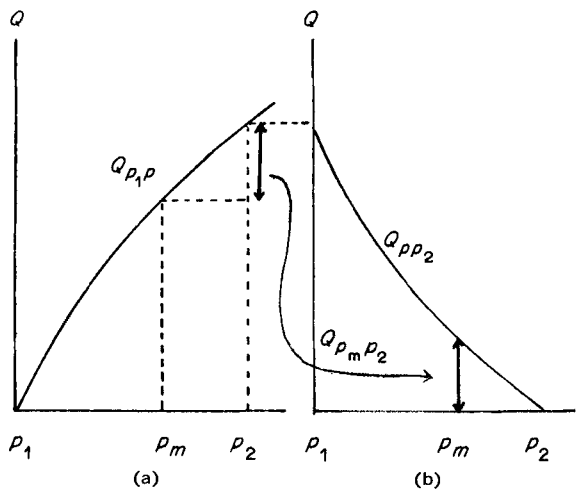

Figure 4—*Rogers' graphical method to obtain* Q_{pp_2} *from* Q_{p_1p}

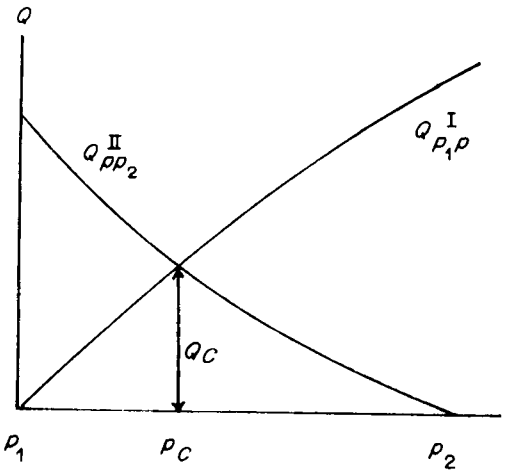

Figure 5—*Graphical estimation of permeability* (Q_c) *of double-layer film composed of Material I (higher humidity side) and Material II (lower humidity side).*

graphically, as shown in Fig. 4, if Q_{p_1p} is given. (This is, in principle, the same method as that used in Table I and/or II.)

Figure 5 gives the combination of $Q^{I}_{p_1p}$ and $Q^{II}_{pp_2}$, where $Q^{I}_{p_1p}$ means the moisture permeability across Film I when the vapor pressure p_1, at the side of higher humidity, is constant with varying vapor pressure p at the lower side. $Q^{II}_{pp_2}$ is Q_{pp_2} of Film II, which is obtained by the method shown in Fig. 4 using the data $Q^{II}_{p_1p}$. Rogers *et al.* (3) indicated that Q_c in Fig. 5 corresponds to the moisture permeability of double-layer film made from I and II, where Film I faces the p_1 side and Film II faces the p_2 side. As a model, Fig. 6 (a and b) illustrates different combinations of films with different moisture permeability characteristics.

Rogers *et al.* (3) explained that the two-sided characteristic of the double-layer film results from the different Q around the intersecting points C and D. When the thicknesses of Films I and II are the same, A, B, C, and D all correspond to the permeability across the films of the same thickness. The characteristics of these double-layer films are classified according to the order of magnitude of Q's around A, B, C, and D as mentioned in an earlier report (1). Figure 6a belongs to group γ, and Figure 6b belongs to group α. Only if the actual data of $Q^{I}_{p_1p}$ and $Q^{II}_{p_1p}$ are given can $Q^{I}_{pp_2}$ and $Q^{II}_{pp_2}$ be determined graphically, where p_2 can be determined to be any value within a range of the mentioned data. For instance, the observed Q_{p_1p} for both ethylcellulose EC-50 of 0.1-mm. thickness and hydroxyethylcellulose acetate phthalate (HECAP) of 0.1-mm. thickness can produce Fig. 7.

Each intersecting point, A, B, C, or D, in Fig. 7 is plotted against humidity conditions to obtain Fig. 8. Figure 8 is utilized to compare the permeation property of the double-layer film with that of each of its single films, where the double-layer film is made from EC-50 and HECAP of 0.1-mm. thickness and single films are EC-50 and HECAP of 0.2 mm. The observed values corresponding to Fig. 8 were plotted in Fig. 9.

When the two graphs are compared, the shapes are seen to be similar, but the predicted graph (Fig. 8) seems to be more compressed in the direction of the ordinate than the observed ones (Fig. 9). These facts may be explained as follows. According to the method of Rogers *et al.* (3) shown in Fig. 4, the moisture permeability is halved when two films of the same kind with the same thickness are piled; that is, the thickness of the film is doubled. In other words, the moisture permeability is inversely proportional to the thickness of the film (or $1/Q$ is in direct proportion to l). Thus, Fig. 4b is obtained when Fig. 4a is turned over symmetrically around the line (parallel to the p ordinate) that passes through the point $^1/_2 \cdot Q$. However, as mentioned in an earlier report (1), the moisture permeability is not exactly in inverse proportion to the thickness but is slightly more than one-half, even if the thickness of the film is doubled. The main reason Fig. 8 differs from Fig. 9 may be attributed to the assumed inversely proportional relation.

Although the following processing method involves some theoretical inadequacies, it may be practically useful to estimate the two-sided property of the double-layer film.

1. The moisture permeability is measured at several Δp levels about single Films I and II, which may be combined to form a

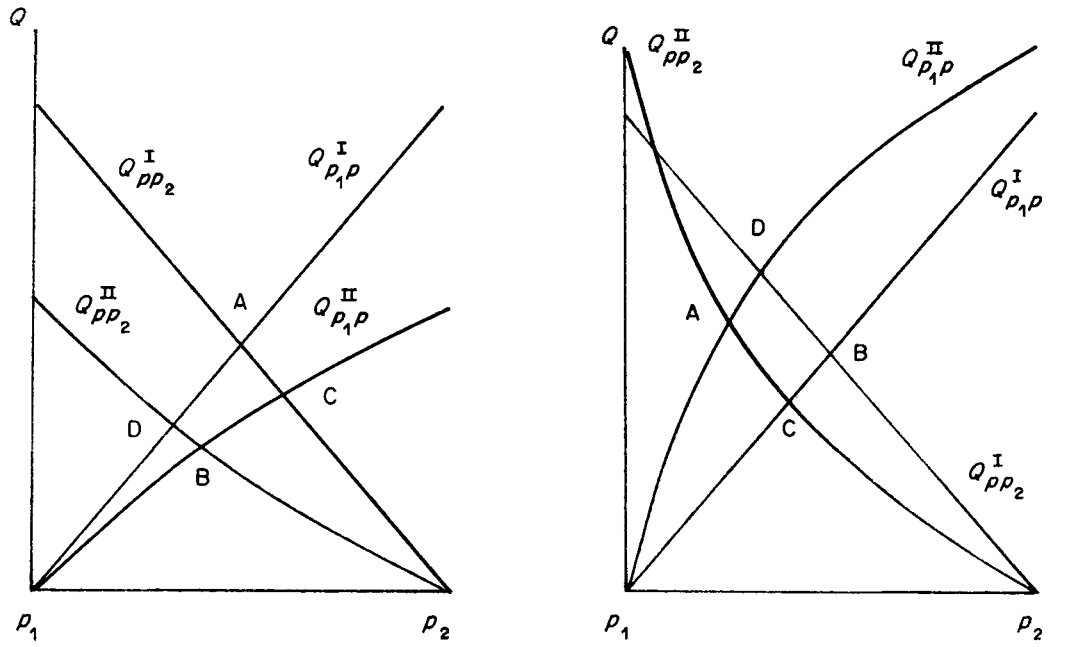

	Film Material	*Water Vapor Pressure (Fixed)*	*Water Vapor Pressure (Varied)*
$Q^{I}_{p_1p}$	*I*	p_1 (*higher pressure side*)	p (*lower pressure side*)
$Q^{I}_{pp_2}$	*I*	p_2 (*lower pressure side*)	p (*higher pressure side*)
$Q^{II}_{p_1p}$	*II*	p_1 (*higher pressure side*)	p (*lower pressure side*)
$Q^{II}_{pp_2}$	*II*	p_2 (*lower pressure side*)	p (*higher pressure side*)

Figure 6—*Two-sidedness of double-layer films (Rogers' method).*

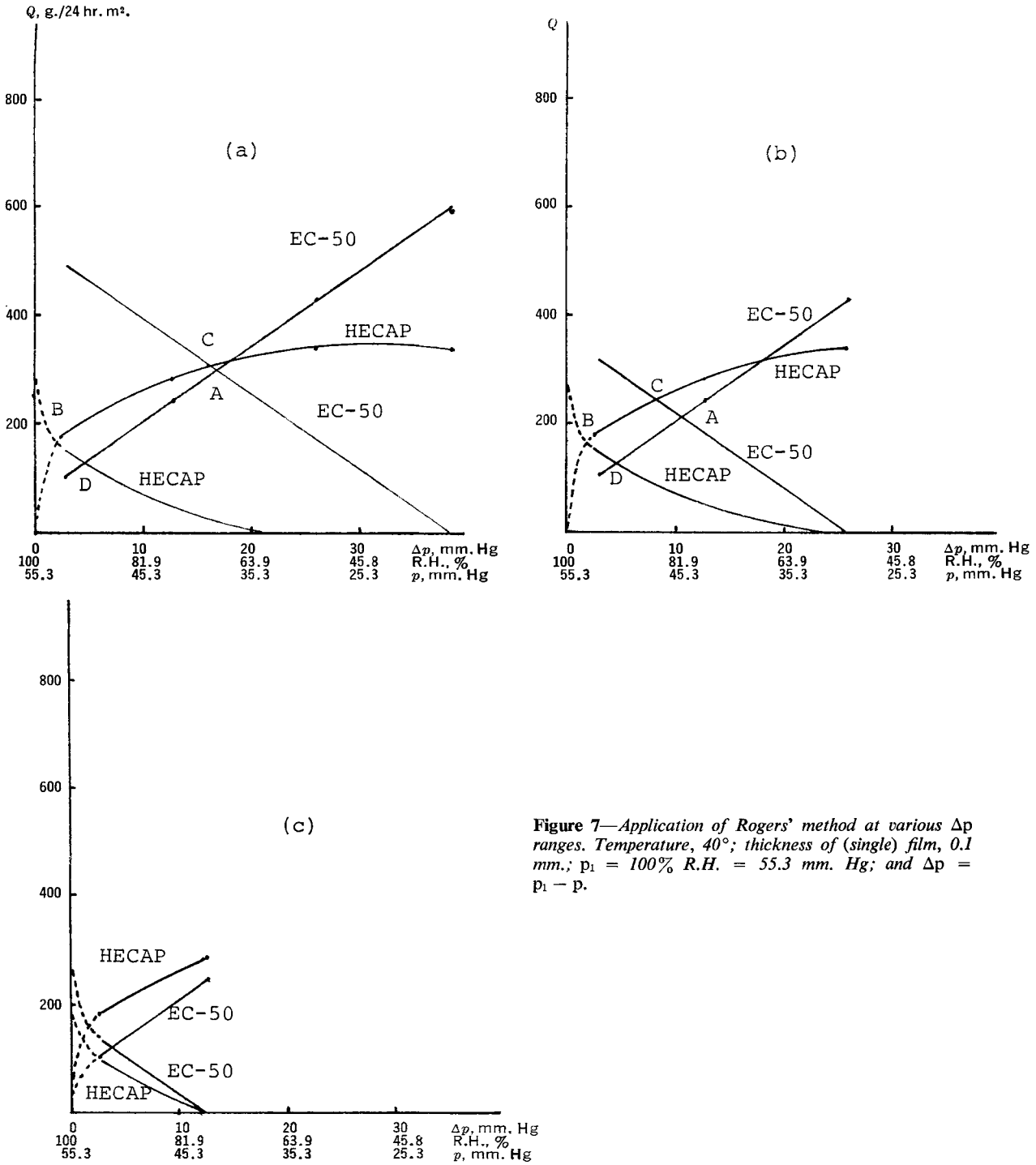

Figure 7—*Application of Rogers' method at various* Δp *ranges. Temperature, 40°; thickness of (single) film, 0.1 mm.;* p_1 = *100% R.H.* = *55.3 mm. Hg; and* Δp = $p_1 - p$.

double-layer film with several levels of thickness. (Although Δp can be set as either $p_1 - p$ or $p - p_2$, the following explanation is carried out using $\Delta p = p_1 - p$.)

2. The data are arranged in terms of: abscissa = l, ordinate = $1/Q$, and parameter = Δp, which afford a linear relationship. The graphs are obtained for I and II.

3. From the graphs obtained in Step 2, the figure is depicted for I and II in terms of: abscissa = Δp, ordinate = Q, and parameter = l. To evaluate the permeability of the double-layer film which consists of I and II when each elemental layer has thickness l_1, the parameter is enough to be l_1 and $2l_1$. In other words, the Q–Δp (or Qp_1p) curve is obtained for both I and II with the thickness l_1 and $2l_1$, respectively.

4. The Q_{pp_2} curve for a given p_2 is obtained by turning the Q_{p_1p} curve of a film with thickness l_1 symmetrically around the line that passes through the point $Q_{p_1p_2}$ of the film with thickness $2l_1$ and is parallel to the Δp axis. The four curves obtained, $Q^{\mathrm{I}}_{p_1p}$, $Q^{\mathrm{I}}_{pp_2}$, $Q^{\mathrm{II}}_{p_1p}$, and $Q^{\mathrm{II}}_{pp_2}$, are drawn in a graph as in Fig. 6.

In this method, different from that of Rogers *et al.* (3), the value of Q along the line of symmetry is not $1/2 \cdot Q_{p_1p_2}$ for l_1 but $Q_{p_1p_2}$ for $2l_1$. From the intersect points in the graph thus obtained, the two-sided characteristic of the double-layer film is evaluated. According to this method, the permeability of any combination of films can be determined only if the data for each single film are given, and the permeabilities of single films can be compared with each other under the same conditions on the any-accurate-thickness (l_1) basis (although it is very difficult to make a film with an exact l_1 thickness). Figure 10 is an example of the result thus obtained with a double-layer film made from EC-50 and HECAP.

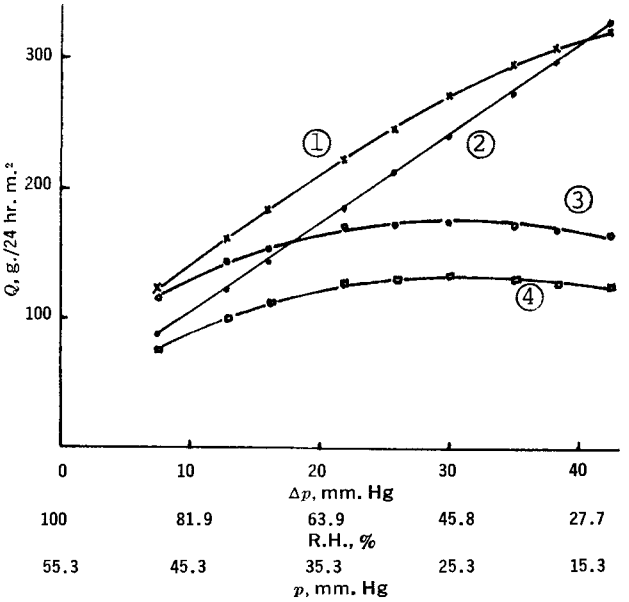

Figure 8—*Estimation of two-sidedness of moisture permeability. Temperature, 40°;* p_1 *= 100% R.H. = 55.3 mm. Hg; and* $\Delta p = p_1 - p$. *Materials:* ①, *HECAP (0.1 mm.) + EC-50 (0.1 mm.);* ②, *EC-50 (0.2 mm.);* ③, *HECAP (0.2 mm.); and* ④, *EC-50 (0.1 mm.) + HECAP (0.1 mm.).*

Figure 10 closely resembles Fig. 9, indicating the usefulness of the method to predict the two-sided property. This graphical method does not necessarily match with the detailed facts. (For instance, $Q^{I}_{p_2p_2}$ does not come to zero.) However, the Q values obtained from the intersecting points make it possible to determine the two-sided property of permeability of the double-layer film with tolerable accuracy.

The differential permeability coefficient can be utilized for another purpose. The $\Delta p/l$ in Eq. 1 is the gradient of vapor pressure across

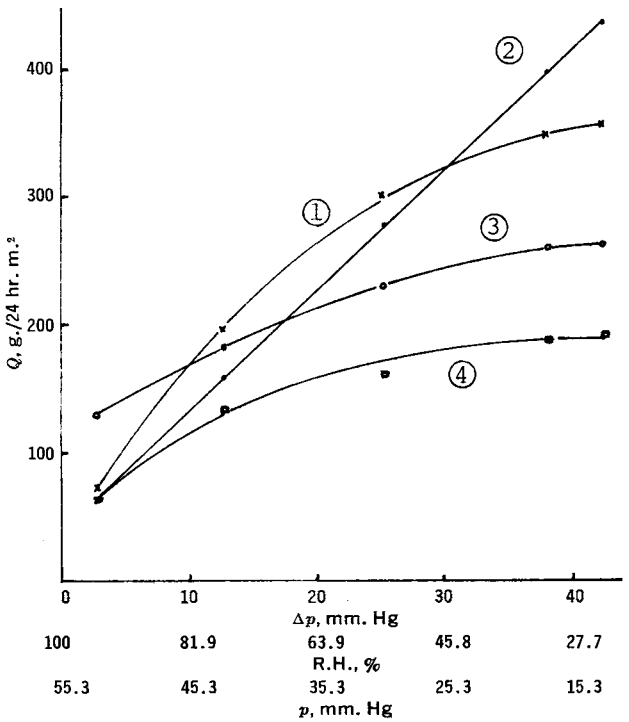

Figure 9—*Two-sidedness of moisture permeability observed. Temperature, 40°;* p_1 *= 100% R.H. = 55.3 mm. Hg; and* $\Delta p = p_1 - p$. *Materials:* ①, *HECAP (0.1 mm.) + EC-50 (0.1 mm.);* ②, *EC-50 (0.2 mm.);* ③, *HECAP (0.2 mm.); and* ④, *EC-50 (0.1 mm.) + HECAP (0.1 mm.).*

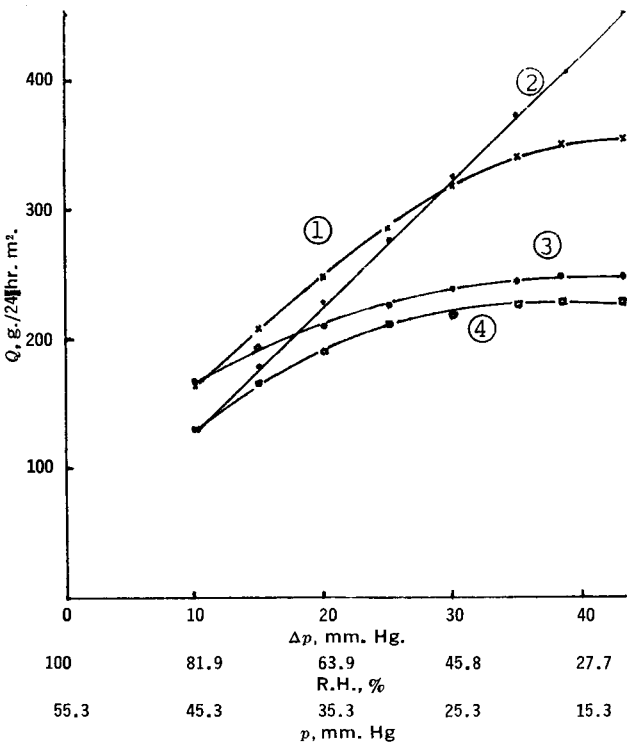

Figure 10—*Estimation of two-sidedness of moisture permeability. Temperature, 40°;* p_1 *= 100% R.H. = 55.3 mm. Hg; and* $\Delta p = p_1 - p$. *Materials:* ①, *HECAP (0.1 mm.) + EC-50 (0.1 mm.);* ②, *EC-50 (0.2 mm.);* ③, *HECAP (0.2 mm.); and* ④, *EC-50 (0.1 mm.) + HECAP (0.1 mm.).*

the film. After permeation arrives at a steady state of condition, the moisture transmitting the cross section of the direction of permeation is of the same quantity as Q, passing through the film itself. Considering the cross section, Eq. 1 then can be written as Eq. 6:

$$Q = -P' \frac{dp}{dx} \qquad \text{(Eq. 6)}$$

where x is the distance from the surface of higher humidity to the aimed cross section of the direction of permeation. This equation may then be correlated to the equation of Fick's law (Eq. 7) on diffusion:

$$Q = -D \frac{\partial c}{\partial x} \qquad \text{(Eq. 7)}$$

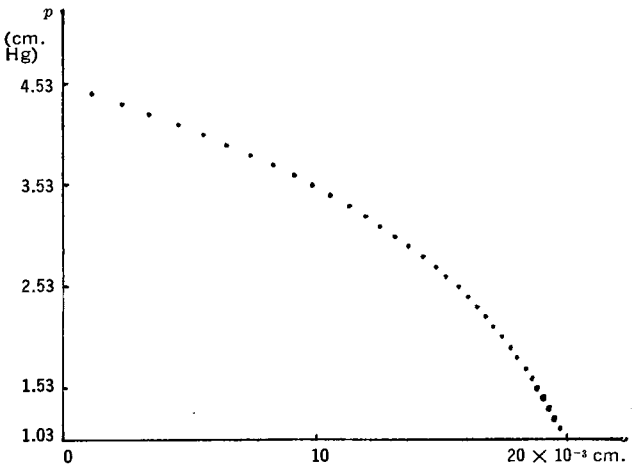

Figure 11—*Water vapor pressure distribution in film (calculated). Film material, MC-25; temperature, 40°;* p_1 *= 4.53 cm. Hg; and* p_2 *= 1.03 cm. Hg.*

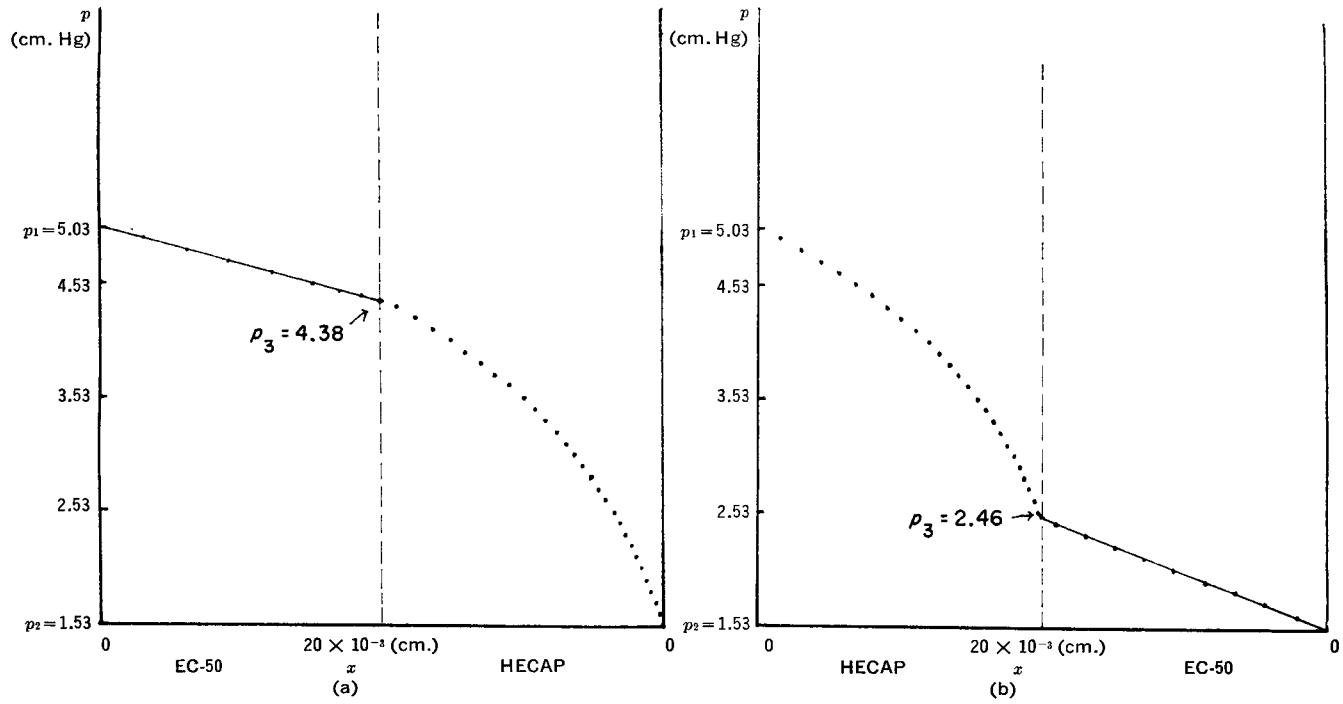

Figure 12—*Water vapor pressure distribution (calculated) of double-layer film. Temperature, 40°;* p_1 = *5.03 cm. Hg; and* p_2 = *1.53 cm. Hg.*

While the diffusion coefficient, D, in Eq. 7 is constant, the differential permeability coefficient, P', in Eq. 6 is a function of the water-vapor pressure. Equation 8 is obtained when Eq. 6 is integrated in the range between $x = 0$ and $x = x$, *i.e.*, between p_1 and p where p_1 = the water vapor pressure at the side of higher humidity, and p = the vapor pressure in equilibrium to cross section across the film ($p_1 > p > p_2$).

$$x = \frac{1}{Q_{p_1p}} \int_{p}^{p_1} P'dp \qquad \text{(Eq. 8)}$$

The distribution of the vapor pressure across the film can be obtained from Fig. 10. Table III shows the calculation process which gives the relation of p to x. This calculation was carried out using the P' value which was calculated in Table I and revised in Fig. 3. These results produce Fig. 11.

The curve of the vapor pressure distribution in MC-25 (hydrophylic film) was concluded not to be linear, although it was linear in the case of a hydrophobic film. Gillespie (6) investigated the water concentration of each layer in some multilayer films and obtained similar results: the curve of water concentration distribution was linear on polystyrene (hydrophobic) and sigmoid on cellophane (hydrophilic). Figure 11 supports this result, although it was not sigmoid. However, Fig. 11 shows the distribution of the vapor pressure; if the vapor pressure distribution is converted into the distribution of water concentration, it will give a sigmoid curve. The reason for this follows. Although the relation of the water vapor pressure, p, to the water concentration, c, which is in equilibrium with the pressure, follows Henry's law (Eq. 9) in general,

$$c = Sp \qquad \text{(Eq. 9)}$$

the relation given by Eq. 10 is valid, as shown by Henley (7) with the propane–polyethylene system, when p varies over a wide range:

$$S = ap + b \qquad \text{(Eq. 10)}$$

where both a and b are constants.

Substituting Eq. 10 into Eq. 9 gives Eq. 11:

$$c = ap^2 + bp \qquad \text{(Eq. 11)}$$

This indicates that c is a function of the second order of p. This has been also supported experimentally by Gillespie (6). The ordinate of Fig. 11 can be converted into the water concentration distribution by using Eq. 11, and then the obtained curve will be more similar to the sigmoid.

Table III—Calculation of Water Vapor Pressure Distribution in Film[a]

p, cm. Hg	P', g./sec. cm. cm. Hg	$\int_{p}^{p_1} P'\,dp$, g./sec. cm.	x, cm.
4.53	445×10^{-11}	0×10^{-11}	0×10^{-3}
4.43	420×10^{-11}	44.5×10^{-11}	1.25×10^{-3}
4.33	400×10^{-11}	86.5×10^{-11}	2.43×10^{-3}
4.23	380×10^{-11}	126.5×10^{-11}	3.57×10^{-3}
4.13	360×10^{-11}	164.5×10^{-11}	4.64×10^{-3}
...	...	...	...
...	...	...	...
...	...	...	...
1.23	76×10^{-11}	694.3×10^{-11}	19.58×10^{-3}
1.13	74×10^{-11}	701.7×10^{-11}	19.79×10^{-3}
1.03	72×10^{-11}	709.1×10^{-11}	20.00×10^{-3}

[a] $p_1 = 4.53$ cm. Hg, $p_2 = 1.03$ cm. Hg, $l = 0.02$ cm., $Q_{p_1p_2} = 1/l \int_{p_2}^{p_1} P'dp = \frac{709.1 \times 10^{-11}}{0.02} = 35.46 \times 10^{-3}$ (g. /sec. cm.^{2}) = 306 (g./24 hr. m.^{2}).

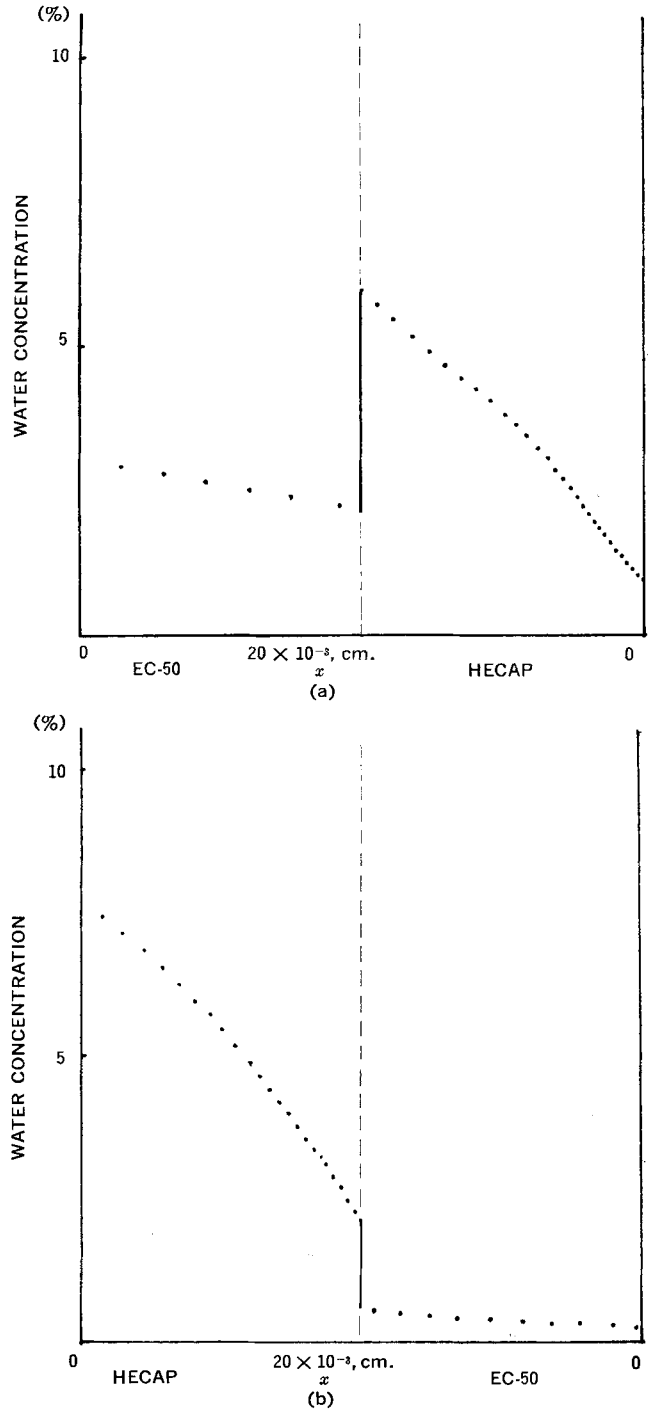

Figure 13—*Water concentration distribution in double-layer film. x = film thickness.*

For a double-layer film of EC-50 and HECAP, the distribution of the water vapor pressure can be shown as in Fig. 12 and the distribution of water concentration can be shown as in Fig. 13. These distributions change, depending upon which side faces the higher humidity atmosphere. In addition, Fig. 13a shows that moisture permeation can occur even against the gradient of water concentration in some cases, although it does not occur against that of the vapor pressure. The curve of the water concentration distribution is not so sharply S-shaped as observed by Gillespie. The difference may be caused mainly by the different experimental conditions between Gillespie's and the present study. Gillespie dealt with multilayer film having air layers between each elemental layer and, of course, the material of the film was different.

SUMMARY

The differential moisture permeability coefficient of a film was actually obtained by calculation. Using this coefficient, the permeability for any humidity condition, not only the condition in which the experiment was actually carried out, can be estimated. The authors introduced a graphical method to estimate the two-sided characteristic of moisture permeability for the double-layer film under changing humidity conditions. In addition, the distributions of both water vapor pressure and water concentration in a film were found to be determined by calculation, even in the case of very thin films for which other determination methods cannot be applied. In hydrophilic films, the curve of the water vapor pressure distribution was not linear. The distribution of the water vapor pressure within the double-layer film with a particularly remarkable two-sidedness was expressed by a specific figure, and the figure changed depending upon which side faced the higher humidity atmosphere. Across the interface of films, moisture permeation was found to occur possibly against the water concentration.

REFERENCES

(1) T. Kuriyama, M. Nobutoki, and M. Nakanishi, *J. Pharm. Sci.*, **59,** 1341(1970).
(2) *Ibid.*, **59,** 1344(1970).
(3) C. E. Rogers, V. Stannet, and M. Szwarc, *Ind. Eng. Chem.*, **49,** 1933(1957).
(4) M. Patel, J. M. Patel, and A. P. Lemberger, *J. Pharm. Sci.*, **53,** 286(1964).
(5) I. Sako, Japanese pat. 438,595.
(6) T. Gillespie, *J. Polym. Sci., Part A-1*, **4,** 933(1966).
(7) E. J. Henley, *AIChE. J.*, **12,** 1030(1966).

ACKNOWLEDGMENTS AND ADDRESSES

Received February 12, 1970, from the *Research Laboratories of Yoshitomi Pharmaceutical Industries, Ltd., Yoshitomi-Cho, Chikujo-Gun, Fukuoka-Prefecture, Japan.*

Accepted for publication April 22, 1970.

Abstracted from a thesis submitted by T. Kuriyama to the Graduate School, Kyushu University, in partial fulfillment of Doctor of Philosophy degree requirements.

Thanks are expressed to Prof. S. Iguchi for his interest in the work and useful discussions; also to Mr. M. Tasaka, Executive Director of Yoshitomi Pharmaceutical Industries, Ltd., for his encouragement and his kind permission to publish this paper.